

# **Microsphere cytometry to interrogate microenvironment-dependent cell signaling**

Henriette C. Ertsås<sup>1</sup>, Garry P. Nolan<sup>2</sup>, Mark A. LaBarge<sup>3</sup> and James B Lorens<sup>1\*</sup>

<sup>1</sup>Department of Biomedicine, Center for Cancer Biomarkers, University of Bergen, Bergen, Norway

<sup>2</sup>Baxter Laboratory in Stem Cell Biology, Department of Microbiology and Immunology, Stanford University, Stanford, CA 94305, USA

<sup>3</sup>Life Science Division, Lawrence Berkeley National Laboratory, Berkeley, CA 94720, USA

## **Abstract**

Microenvironmental cues comprising surface-mediated and soluble factors control cellular signaling mechanisms underlying normal cellular responses that define homeostatic and diseased cell states. In order to measure cell signaling in single adherent cells, we developed a novel microsphere-based flow cytometry approach. Single normal or neoplastic cells were adhered to uniform microspheres that display mimetic-microenvironments comprising surface combinations of extracellular matrix (ECM) in the presence of soluble agonists/antagonists. Temporal signaling responses were measured with fluorophore-conjugated antibodies that recognize response-dependent epitopes by multiparametric flow cytometry. Using this approach we demonstrate that microenvironment-mimetic combinations of growth factors and extracellular matrix proteins generate distinct cellular signal networks that reveal unique cell signatures in normal and patient biopsy-derived neoplastic cells.

## **Insight, innovation, integration**

Modern multiparametric flow cytometry enables quantitative analysis of cell signaling pathways at a single-cell level within heterogeneous populations by simultaneously detecting both intracellular and extracellular epitopes on individual cells. A limitation of this approach, however, is that adherent cells must be detached to adopt the suspended, spherical conformation required for laminar flow fluidics, a non-native state for adherent cell types that dramatically affects signaling states. We have developed a novel approach using bio-functionalized polystyrene microspheres to allow single cell analysis in the context of mimetic microenvironments by flow cytometry. This convenient system is amenable to any adherent cell type and can provide unique mechanistic insights into how surface mediated microenvironmental cues regulate signal transduction and reveal altered cell responses in heterogeneous cell systems.



## **Introduction**

Cellular context is defined by combinatorial cell signaling mechanisms that integrate signal transduction networks. Microenvironmental cues comprising hetero- and homotypic cell-cell interactions, extracellular matrix-integrin engagement, tissue modulus, oxygen tension and cytokines/growth factors activate cellular signaling mechanisms that determine cellular phenotypes such as lineage decisions during development and tissue homeostasis in the adult<sup>1,2,3</sup>. Adherent cells require attachment to extracellular matrix (ECM) via integrins for survival and normal function<sup>3</sup>. The cellular integrin repertoire mediate tissue specific ECM information to adherent cells, affecting responsiveness to soluble factors and determining contextual cell signaling<sup>4</sup>.

Cellular signal transduction generates unique response-dependent protein modifications, such as phosphorylation, that can be detected by specific antibodies and quantified at the single cell level by flow cytometry approaches<sup>5</sup>. Signaling heterogeneity within cell populations reveals molecular profiles associated with the pathogenesis and clinical outcome<sup>6</sup>. A limitation of current flow-based methods is that cells must adopt a spherical configuration to enter the laminar flow system. Hence, adherent cell types must be released from growth substrates prior to analysis confounding signal transduction analysis. To address this, we developed a microsphere cytometry approach to enable flow cytometric analysis of signaling in phenotypes of adherent cells in defined microenvironmental contexts. Single normal or neoplastic cells are adhered to uniform microspheres that display various biofunctionalized surfaces (e.g. ECM proteins or receptor ligands) and exposed to selected combinations of soluble agonists/antagonists (e.g. growth factors, cytokines, hormones, small molecules). Using this approach we have measured the effects of microenvironment-mimetic combinations of surface-mediated and soluble factors on adherent cell signal networks at the single cell level and identified unique signaling-based biomarkers of cancer cells.

## Results

### Quantifying adherent cell signaling at the single cell level by flow cytometry

In order to study signaling events in single cells in defined microenvironmental contexts we exposed cells to substrata that enabled cell adhesion and was compatible with flow cytometry. Uniform 20  $\mu\text{m}$  diameter polystyrene microspheres provide a surface area of  $1256 \mu\text{m}^2$ , are sufficiently large to support adhesion of an average single cell, and are compatible with flow cytometry systems. Immortalized human mammary epithelial cells (MCF10A) attached to microspheres coated with collagen type I (COL1). Subsequently, epithelial cell-microsphere complexes were fixed and analyzed by electron microscopy to observe the adhesion process in progress. As shown in Fig. 1A, the human epithelial cells initially adsorbed to the microsphere surface and gradually adhered by forming filopodia that spread over the majority of the available microsphere surface. To further characterize this cell attachment to a curved surface, we analyzed F-actin fibers in MCF10A cells bound to COL1-coated microspheres by 3D confocal image analysis. Phalloidin-stained actin fibers were evenly distributed throughout the cell and the entire circumference of the microsphere surface (Suppl. Fig.1A; Supp. Movie 1). This analysis suggests that cells form attachments to ECM-coated microspheres in a fashion similar to flat tissue culture surfaces congruent with previous reports<sup>7</sup>. In order to analyze cell signaling in single microsphere-adhered cells, we developed a flow cytometry protocol schematically displayed in Fig 1B. Microspheres coated with different ECM proteins (COL1, laminin (LAM) and fibronectin (FN) showed a uniform staining with anti-ECM antibodies by flow cytometry (Suppl. Fig.1B). A mix of paraformaldehyde-fixed MCF10A cells, microspheres and MCF10A cells bound to COL1-coated microspheres were analyzed by flow cytometry. Microspheres were resolved by a characteristic high light side scattering value (SSC); whereas unbound and microsphere-bound cells were identified by DNA staining with propidium iodide (PI). The gating strategy (SSC-A vs SSC-W, FSC-A vs DNA-staining) was designed to enrich cells having similar microsphere-attachment geometry (Fig.1C-D). The microsphere-adhered cells were compatible with flow sorting, and microscopy analysis confirmed the

identity of the different populations (Fig. 1C). The percentage of microsphere-bound cells with  $>4n$  DNA content was indistinguishable from the unbound cell population, indicating a 1:1 cell-microsphere ratio (Fig. 1D). Importantly, this DNA content analysis demonstrated that cell-microsphere orientation relative to the incident laser beam or the position of photomultiplier tube detector did not significantly influence fluorescence signal strength relative to cells in suspension (Fig.1D). Cell adhesion kinetics to different biofunctionalized microspheres varied by cell type. MCF10A cells displayed similar rapid saturating attachment kinetics to COL1, LAM and FN (Fig. 1E), but MDA-MD-231 breast carcinoma cells showed delayed attachment to FN (Suppl. Fig.1C).

We next determined if signaling events could be detected in cells attached to microspheres. Phosphorylated extracellular signal regulated kinase (pERK) was measured in NIH3T3 fibroblasts adhered to COL1-coated microspheres, stimulated with serum or phorbol 12-myristate 13-acetate (PMA). The activated microsphere-bound fibroblasts were fixed, permeabilized and stained with anti-pERK antibodies using an established phosphoflow protocol<sup>5,8</sup>. Flow cytometry analysis of the microsphere-bound fibroblast population showed a strong induction of pERK by serum and PMA treatment (Fig. 1F). The presence of serum reduced the extent of PMA-mediated pERK induction, attributable to the serum protein binding of PMA<sup>9</sup>. Taken together, microsphere cytometry enabled FACS-based detection of ECM-dependent adhesion behaviors and signaling activities in a number of stimulatory conditions.

### **Simultaneous measurement of cell signaling responses in adherent and non-adherent monocytes**

Monocytes can assume either an adherent or non-adherent phenotype in a basic fibroblast growth factor (FGF2) dependent fashion<sup>10</sup>. The monocytic cell line U937 and primary human CD14<sup>+</sup> monocytes are cultured in suspension, but acquire a macrophage-like fibronectin-adherent phenotype following 7-hours of treatment with FGF2<sup>10</sup>. We compared MAPK (pERK), PI3K-AKT (pAKT), JAK-STAT (pSTAT3/5) and PKC (pMARCKS) pathway activation simultaneously in single FN-adhered and non-adherent monocyte cells in response to FGF2, PMA, granulocyte-macrophage colony-stimulating factor

(GM-CSF) or IL-6 treatment (Fig.2A). PMA treatment (50  $\mu$ M, 2 minutes) potently activated pERK and pMARCKS both in bound and unbound monocytes, while FGF2 (100 ng/ml, 15 minutes) did not induce detectable effects. GM-CSF and IL-6 activated pSTAT5 and pSTAT3 in both bound and unbound U937 monocytes. In general, microsphere-bound monocytes showed reduced basal phosphorylation levels, but similar activation compared to cells in suspension or unbound cells (Fig.2). pAKT levels were low throughout the experiment likely due to negative feedback received from the MAPK pathway<sup>11</sup>. Collectively, these results validate that the microsphere cytometry approach provides a unique opportunity to simultaneously profile signal transduction in adherent and suspended cells within the same sample, which is particularly useful for cell types like monocytes that adopt both states in vivo.

### **Contextual cell signaling responses to ECM in mammary epithelial cells**

In order to quantify epithelial cell signaling responses to different ECM at the single cell level, MCF10A cells were bound to different ECM-coated microspheres for 3 hours, incubated in serum/growth factor-free medium for 50 minutes, and then stimulated with PMA, EGF or 5% serum. pERK and pAKT levels were measured in single microsphere-bound epithelial cells (Fig.3, Supp. Table 1). EGF and serum stimulated pERK and pAKT in an ECM-dependent manner. MCF10A displayed higher pERK and pAKT levels following growth factor activation when bound to FN and LAM. In contrast, EGF induced pERK and pAKT levels in MCF10A cells bound to collagen IV (COL4) microspheres remained indistinguishable from unstimulated cells, indicating that COL4 represses EGF signaling. PMA treatment bypassed contextual ECM input, activating pERK equivalently irrespective of the substrate. Thus the microsphere approach can reveal contextual differences in signaling pathways in single cells.

### **Microenvironment contextual cell signaling response patterns distinguish normal and neoplastic cells**

A hallmark of cancer cells is altered cell signaling responses to microenvironmental signals. We reasoned that cell signal transduction dynamics in single carcinoma cells, measured by longitudinal sampling of cells

adhered to different ECM-coated microspheres, would provide a unique perspective of contextual signaling responses that distinguish cancer cell phenotypes. We generated immortal HMEC by co-expressing ectopic CCND1 and cMyc<sup>12</sup> followed by malignant transformation by overexpressing ERBB2/Neu. The HMEC/Neu and the isogenic normal parental HMEC strain, together with non-tumorigenic MCF10A and malignant MDA-MB-231 triple negative breast cancer cells, were interrogated for cell signaling differences when adhered to three different ECM contexts. Microsphere-bound cells were sampled at different time points (10 min - 9 hr) and single cell pERK/ pAKT levels were measured to monitor MAPK/PI3K-AKT response kinetics (Fig. 4A,B).

As shown in Fig 4D, normal HMEC adhered to COL1, FN and LAM-coated microspheres in the presence of EGF supplemented growth medium, displayed a rapid, transient pAKT (dotted line) increase, reaching a maximum approximately 30 minutes post-adherence, when ERK activation initiated. This reciprocal AKT/ERK activation pattern was apparent in HMEC adhered to all three ECM substrates. Both pERK and pAKT levels decayed to low basal levels by 9 hours on COL1 and FN, but remained elevated in HMEC adhered to LAM (Fig.4E). In contrast, HMEC/Neu cells showed coordinated and transient AKT and ERK activation that resolved to stable basal phosphorylation levels (Fig 4E). The MCF10A cells showed an intermediate signaling phenotype with an early reciprocal AKT/ERK activation, similar to normal HMEC (Fig 4B). However, unlike normal HMEC, MCF10A sustained pAKT and pERK levels that were higher than basal levels for as long as 9h after attachment to the microspheres (Fig 4E). MDA-MB-231 cells showed high constitutive pERK levels with short term bursts of activation, the shapes of which varied on the different ECM (Fig 4D). In contrast to the other cell types, MDA-MB-231 had overall lower pAKT levels in all conditions compared to the other cell types. Collectively these results show that adhesion-dependent signaling dynamics varied strongly between normal and transformed epithelial cells.

To further characterize the nature of the observed reciprocal AKT/ERK activation pattern, we analyzed crosstalk between MAPK and PI3K-AKT

pathways in growth factor stimulated MCF10A after 2 hours of serum starvation in cells adhered to different ECM-coated microspheres (Fig 4C). In the absence of growth factors, mere adhesion to the ECM-coated microspheres upregulated pAKT, with FN inducing the highest level (Fig. 5A). Addition of EGF, led to pERK stimulation with the highest level found in LAM-bound cells, while pAKT levels were comparable among the different ECM-bound MCF10A cells (Fig 5A). PMA treatment generated pERK upregulation accompanied by reduced pAKT levels (Fig 5A). Treatment with the EGFR kinase inhibitor AG1478 (80nM) blocked EGF-stimulated pERK on LAM, without affecting pAKT levels (Fig 5B). Inhibition of PI3K (wortmaninn, 500nM) completely abrogated the pAKT response under all conditions (Fig 5C). Notably, also EGF-induced pERK levels were abrogated, while PMA-stimulated adherent cells displayed pERK activation. Direct inhibition of AKT with an allosteric inhibitor (AKTVIII, 10uM) blocked pAKT while actually allowing some activation of pERK due to the removal of inhibitory regulation of MAP kinase by pAKT (Fig 5D). Conversely, treatment with the MEK inhibitor PD98059 (10  $\mu$ M), blocked EGF-stimulated pERK without altering pAKT, while PMA-induced AKT/ERK activation was unaffected (Fig 5E). These results reveal contextual differences in epithelial MAPK/PI3K-AKT signaling connectivity endowed by ECM.

### **Microsphere cytometry analysis of primary tumor biopsies**

Next we applied the microsphere cytometry approach to measure signal transduction profiles in patient-derived ovarian carcinoma cells from an abdominal ascites biopsy. Tumor cells were isolated from the heterogenous fresh ascites fluid by EpCAM FACS sorting and short-term culture in low stress M87+oxytocin medium<sup>13,14</sup>. Laminin-coated microspheres were then added to the ovarian carcinoma cell-enriched sample for 7 hours. An aliquot was taken and treated with EGF for 20 minutes prior to phosphoflow analysis. The ascites-derived primary ovarian carcinoma cells displayed a strong pAKT response to EGF treatment, while pERK was relatively unchanged compared to basal levels (Fig. 6A). Next, we examined ascites-derived primary ovarian carcinoma cells enriched via serial partial trypsination and adhered to COL1-coated microspheres. Ovarian carcinoma cells bound readily to COL1-coated microspheres in the presence of EGF-supplemented medium (Fig.6B). We

measured pERK levels in the COL1-microsphere bound ovarian carcinoma cells after 10 min and up to 4 hours. The COL1-microsphere bound ovarian carcinoma cells showed pERK activation upon binding to the COL1-microspheres that attenuated after 2 hrs. A mixed basal and activated pERK subpopulation manifested at 4 hours within the COL1-microsphere bound primary ovarian carcinoma cells, congruent to that observed for the normal HMEC (Fig 4A). These results indicate that the microsphere cytometry approach can uniquely measure signal transduction profiles in primary patient biopsy-derived cancer cells.

## Discussion

Adherent cell states are determined by adhesion receptor crosstalk with growth factor receptor signal transduction. Contextual growth factor responses in different ECM microenvironments are the result of coordinated integrin-RTK crosstalk that affects shared downstream signal transduction. Matrix-ligated integrins can regulate RTK signaling at multiple levels including activation of signaling kinases and phosphatases, via direct physical interaction and by affecting surface receptor recycling<sup>15–17</sup>. Integrin-signaling complexes mediate both phosphorylation and dephosphorylation of tyrosines on RTK intracellular domains that affect signaling thresholds, while RTK signaling can modulate integrin expression levels.

Microsphere cytometry provides a unique method to measure combined matrix- and growth factor-mediated temporal signaling dynamics in single adherent cells. Using this approach we show a way forward for dissecting the relative roles of context and intrinsic cellular states in signaling responses, as exemplified by our study of multiple mammary epithelial cells that ranged from normal to malignantly transformed (Fig. 4). The mammary epithelial cell line MCF10A exhibited unique patterns of serum and growth factor signaling responses when adhered to different ECM-coated surfaces (Fig.3). The MAPK and PI3K-AKT signaling pathways control cell survival, differentiation, proliferation, metabolism, and motility in response to extracellular cues. EGF-stimulated MAPK and PI3K-AKT pathway activation in epithelial cells adhered

to COL1, LAM, VN and FN. However, adhesion to COL4 strongly suppressed responsiveness to EGF stimulation (Fig. 3). Such negative regulation of receptor tyrosine kinase signaling has been attributed to integrin activation of phosphatases<sup>15</sup>. Interestingly, COL4-adhered cells showed lower pAKT levels in the presence of EGF than without, suggesting that EGFR stimulation may reduce integrin-mediated AKT activation in this context. COL4 and LAM are major components of the mammary basement membrane that maintain tissue integrity. Our data indicate that COL4 and LAM contribute to tissue homeostasis in part by regulation of contextual cell signaling responses.

Cell signaling dynamics can provide unique insight into cell states. Kinetic analysis of EGF-stimulated HMEC adhered to different matrixes revealed a reciprocal MAPK and PI3K-AKT activation profile indicative of strong pathway crosstalk. The MAPK and PI3K-AKT pathways regulate each other at multiple points, comprising both positive and negative feedback loops<sup>18–20</sup>. We observed that ERK activation was delayed until pAKT levels reached a maximum; pERK then increased as pAKT levels decayed. These results are congruent with our observation that cellular context regulates endothelial cell Akt protein dynamics that determine MAP kinase signaling thresholds necessary to drive a morphogenetic program during angiogenesis<sup>21</sup>.

Matrix-adhered normal, transformed and malignant epithelial cells displayed distinctive signaling dynamics that are reflective of altered signaling landscapes. Whereas MAPK and PI3K-AKT pathways were reciprocally regulated in normal (HMEC) and in immortally transformed MCF10A cells, their activation was largely decoupled in the malignant cells (HMEC/Neu and MDA-MB-231). We assume these differences arose because of cognate oncogenic mutations e.g. HER/Neu overexpression in HMEC/Neu and KRAS in MDA-MB-231. It is of note that MCF10A are commonly denoted as “normal” mammary epithelial cells, in spite of the fact that they are immortally transformed and aneuploid. The microsphere kinetic analysis here reveals that MCF10A differ from normal HMEC, in that once AKT and ERK were stimulated by different ECM they did not return to a basal state within the 9h timeframe of the experiment, unlike the normal pre-stasis HMEC. These characteristic temporal



signaling profiles could be used to distinguish tumor cells with more aggressive characteristics. Accordingly, we have shown the feasibility of using microsphere cytometry for this by analyzing adherent cell signal transduction dynamics in conjunction with immune phenotyping of primary ovarian carcinoma cells in ascites biopsies.

We used small molecule inhibitors to block specific signaling proteins to reveal inter-relationships between adherent cell signaling pathways. PI3K inhibition completely abrogated epithelial pERK and pAKT responses to ECM and growth factors, while PMA rescued ERK activation. In contrast, an AKT1/2-selective allosteric inhibitor, which effectively blocked pAKT induction, was selectively rescued by PMA treatment of FN-adherent cells. As the pAKT antibody does not distinguish between the three AKT isoforms, the pAKT signal may be attributed to AKT3 activation by PMA. MEK inhibition blocked EGF-stimulated pERK activation without altering pAKT. These results implicate PI3K as a key integrator of the MAPK and PI3K-AKT pathways in this system.

Microsphere cytometry provides a valuable alternative to microscopy-based methods to study adherent cell types. The method can be conducted on a standard flow cytometer that in general allows better quantification of multiple cellular response parameters at the single cell level. Further, FACS provides the opportunity to isolate specific cell-microsphere populations based on specific features (Fig. 1)<sup>22,23</sup>. Our preliminary results indicate that microsphere cytometry is amenable to mass cytometry instrumentation (data not shown), that will dramatically expand the breath of cellular parameters (>40) available to interrogate single adherent cells<sup>24,25</sup>. Imaging cytometry methods uniquely facilitate measurement of morphological and spatial information<sup>24</sup>. The microsphere cytometry proved useful for kinetics experiments measuring signaling transduction taking place over minutes and hours. Earlier stages of the pathway, such as phosphorylation of receptors further upstream passes within seconds and would require other methods, for instance Digital microfluidic Immunocytochemistry in Single Cells (DISC)<sup>27</sup>.

Collectively, we demonstrate that the microsphere cytometry approach facilitates interrogation of microenvironmental effects on signal transduction dynamics in adherent cells that can reveal clinically relevant insight into contextual cell states. The opportunity to apply this method to patient biopsy material may provide novel biomarkers of therapeutic responses.

## **Experimental**

### **Microspheres**

VARIAN PL-Microspheres SuperCarbonyl White poly(styrene-co-methacrylic acid) 20 µm in diameter, (Batch CD185, Polysciences Inc.)

### **Coating of microspheres with ECM proteins**

*COL1 and COL 4 coating:* A 500 µL microsphere suspension was washed twice with 1 mL 0.01 M HCl and centrifuged at 390 g for 2 min. 1.5 mL COL1 from rat tail (1mg mL<sup>-1</sup>, Sigma-Aldrich #C7661) or COL4 from human placenta (2mg mL<sup>-1</sup>, Sigma-Aldrich #C5533) was added dissolved in 0,1M acetate. The microsphere was placed on a carousel at 4°C for 48 hours, then pelleted at 390g for 2 min. Microspheres were washed twice with serum free medium followed by a blocking step of 2 mL 1% Bovine Serum Albumin (Sigma Aldrich #A9647) in PBS, on a carousel at 4°C for 24 hours.

*FN, Vitronectin (VN) and LAM:* 500 µl microsphere suspension was washed three times with PBS. 1 mL of a 7.5 µg mL<sup>-1</sup> solution was added of either FN from bovine plasma (Sigma-Aldrich # F1141) or VN (Upstate #08-126) in a PBS suspension or LAM from Engelbreth-Holm Swarm murine sarcoma (Sigma-Aldrich #L2020) in acetate buffer (100 mM acetate, 0.05% Triton-100, 20% glycerol, pH 5.3). The microsphere mix was placed on a carousel at 4°C for 24 hours. All microspheres – independent of coating – were finally washed twice with serum free medium and resuspended in cell medium to a concentration of 22.5 x10<sup>6</sup> microspheres mL<sup>-1</sup>

### **Cell culture**

MCF10A and MDA-MB-231 cells were obtained from American Type Culture Collection (Rockville, MD). MCF10A cells were cultured in medium previously described<sup>28</sup>. MDA-MD-231 cells were cultured in Ham's F12 medium (Sigma Aldrich) supplemented with 1mM L-Glutamine, 10% fetal bovine serum (Euro Clone, PAA), 100U mL<sup>-1</sup> Penicillin and 100µg mL<sup>-1</sup> Streptomycin<sup>29</sup>. Finite life span mammary epithelial cells were obtained from reduction mammoplasty of a 19 year old woman (240L)<sup>30</sup>. Cells were cultured in M87A medium (1:1 mix of medium MCDB 170 (Gibco) and DMEM/F12 (Sigma-Aldrich) ) supplemented

with 7.5  $\mu\text{g mL}^{-1}$  insulin, 35  $\mu\text{g mL}^{-1}$  bovine pituitary extract, 5  $\text{ng mL}^{-1}$  EGF, 2.5  $\mu\text{g mL}^{-1}$  Apo-transferrin, 5 nM isoproterenol, 2.0 mM L-Glutamine, 5 nM tri-iodothyronine,  $0.5 \times 10^{-10}$  M  $17\beta$ -estradiol, 0.3  $\mu\text{g mL}^{-1}$  hydrocortisone, 0.25% fetal calf serum, 0.1% AlbuMAX, 100U  $\text{mL}^{-1}$  penicillin and 100 $\mu\text{g mL}^{-1}$  streptomycin supplemented with 0.5  $\text{ng mL}^{-1}$  cholera toxin and 0.1 nM oxytocin<sup>14</sup>. Phoenix A retroviral packaging cells were grown in DMEM supplemented with 1mM L-Glutamine, 10% fetal bovine serum, 100U  $\text{mL}^{-1}$  penicillin and 100 $\mu\text{g mL}^{-1}$  streptomycin<sup>31</sup>. The monocytic U937 cell line (ATCC) was cultured in RPMI 1640 medium supplemented with 10% Fetal Calf Serum, 25 mM HEPES, 25 nM  $\text{NaHCO}_3$ , 1nM L-Glutamine, 100U  $\text{mL}^{-1}$  penicillin and 100 $\mu\text{g mL}^{-1}$  streptomycin. Terminal monocytic differentiation was induced in U937 as described by Weston et al<sup>10</sup>, with 20  $\text{ng mL}^{-1}$  FGF2 (R&D233-FB025) treatment for 10 hours, of which 7 hours were in the presence of FN coated microspheres. The population referred to as suspension cells were equally treated with FGF2 but no microspheres were introduced. Peripheral blood mononuclear cells (PBMC) were isolated from whole blood by gradient centrifugation using Lymphoprep<sup>32</sup>. Primary monocytes were isolated from PBMC by introducing microspheres, due to selective adsorption. Adherence to microspheres was induced by treating the PBMC sample with FGF2 as described above. Monocytic identity was confirmed by staining for CD14 positivity (1:10, Invitrogen #MHCD1400), only CD14 positive cells were included in the analysis. Cells were serum-starved for 18 hours upon stimulation. Erythrocytes and platelets remained in suspension and were gated out during data analysis.

### **Retroviral Transduction of HMEC**

We generated isogenic immortalized and oncogenic cell lines from a HMEC strain (19y). Packaging 293T cells were co-transfected with GFR-tagged CyclinD plasmid construct (pLVTH, Didier Trono, Addgene plasmid #312262) and helper plasmids expressing the structural proteins (gag-pol and env) needed to form functioning virus. The transfection mix contained: 1.7  $\mu\text{g}$  CyclinD construct or empty vector control construct, 2.8  $\mu\text{g}$  M334(GAG-pol) and 0.5  $\mu\text{g}$  M5(VSV) followed by 15  $\mu\text{L}$  Fugene HD in a total volume of 500  $\mu\text{L}$  OptiMEM 1 (without serum and antibiotics). The mix was incubated for 15 min. at room temperature and added dropwise to 293T cells in a 10 cm cell culture

dish containing 8 ml of preferred culture medium. The harvested 293T supernatant containing lentivirus was filtered through a 0.45  $\mu\text{m}$  filter and stored at  $-80^{\circ}\text{C}$ . Protamine sulphate ( $5 \mu\text{m mL}^{-1}$ , Sigma-Aldrich #P4020) was added to thawed filtrate and used to transduce passage 3 HMEC. Transduced cells were enriched by cytometric sorting on a FACS Aria (BD biosciences) based on GFP expression.

Secondly cMyc was introduced in a retroviral vector for cells to overcome telomere dysfunction and become immortal. Subconfluent phoenix packaging cells in a six well plate were transfected with calcium-precipitated vectors (cMyc gene in a pBABE vector, Neu/Her2 in pWZL Blast ST, Addgene plasmid #13805) as described by Swift 2001<sup>31</sup>. Virus harvesting was initiated 25 hours post transfection, when target cell media was applied. Virus collected within the following 21 hours was sterile filtrated through a 0.45  $\mu\text{m}$  filter and supplied with protamine sulphate ( $5 \mu\text{m mL}^{-1}$ , (Sigma-Aldrich #P4020). Subconfluent Cyclin D1 transduced HMEC target cells (passage 4) seeded into six well plates received a spin-infection (1200g for 90 min.) followed by incubation over night. cMyc pBABE vector -transduced cells were selected with hygromycin ( $10\mu\text{g mL}^{-1}$ , Sigma-Aldrich #3274). Empty vector transduced cells would eventually go into senescence around passage 16 which is the maximum number of passages normally obtained for finite life cells. Growth curves were kept to detect when cells no longer grew.. CyclinD/cMyc positive cells survived beyond passage 20 and was defined as immortal. Immortal CyclinD/cMYc HMEC were transduced with Neu/Her2 to create anchorage independent cells. Anchorage independence is a well-known cancer hallmark and was confirmed by anchorage independent assay. Transduced cells were selected by Blasticidin ( $10\mu\text{g mL}^{-1}$ , Sigma-Aldrich #15205)

### **Anchorage independent assay**

---

Each well in a six well plates were coated with with 0.7 mL 0,6 % agarose incubated in RT for 30 min. Methyl cellulose (Sigma #M0512) was freshly prepared with M87A complete medium. 1,5 g methyl cellulose (Sigma #M0512) was autoclaved for 20 min. and then dissolved in 100ml warm media

(37°C) with a stirring bar. The suspension was dissolved overnight at 4°C with continuous stirring. The solution was then centrifuged at 4000g for 30 minutes, to pellet any undissolved methyl cellulose. The supernatant was poured into a new container and handled at 4°C in order to stay sufficiently fluid. One part of cell suspension ( $1 \times 10^5$  cells  $\text{mL}^{-1}$  medium) was diluted in four parts of methyl cellulose and added to the six well plate. 1 mL of final mix went into each well in duplicates. Additional methyl cellulose was added once a week to replenish the necessary nutrients. Colonies exceeding a minimum diameter of 80  $\mu\text{m}$  were registered after 4 weeks. Normal cells do not survive long without the opportunity to make molecular connections with their surroundings. Methyl cellulose gel does not allow such connections; only anchorage independent cells will survive and proliferate into cell aggregates.

### **Cell cycle analysis**

Microsphere bound cells and cold trypsinized cells in suspension<sup>33</sup> were pretreated with Ribonuclease I ( $100 \mu\text{g mL}^{-1}$ , Sigma-Aldrich #R4875) and then stained directly with Propidium iodide (PI) into solution (Sigma Aldrich #P4864) at a final concentration of  $50 \mu\text{g mL}^{-1}$  for 15 min. Samples were run directly on the BD FACSAria (BD Biosciences).

### **Microsphere Cytometry protocol**

Cultured cells were washed twice with PBS and treated with low concentration trypsin (0.05% trypsin, 0.02% EDTA in PBS) until just detached. Suspended cells were mixed with microspheres at a ratio of  $7.5 \times 10^5$  cells to  $22.5 \times 10^5$  microspheres in a total volume of 300  $\mu\text{l}$  and incubated on a shaker for 45 min at 37°C. Cell culture medium (10 mL) with serum was added, the mix was transferred to a sterile bacterial petri dish and incubated for 2-4 hour to allow cells to attach to the microspheres depending on the cell type and type of ECM coating. Cell-microsphere complexes were pelleted at 390g for 2 min, 10 ml serum-free medium was added and the cell-microsphere complexes were then serum-starved for 30 min. in order to achieve a low base phosphorylation level and synchronize activation levels cells in the sample. U937 and primary monocytes were starved overnight. Finally, cell-microsphere complexes were vortexed and pelleted at 130g for 5 min. in preparation for stimulation. Cells

were stimulated with: FGF2 (100 ng mL<sup>-1</sup> , 15 min., R & D #233-FB025), PMA (50 µM, 2 min, Sigma-Aldrich #P1585), GM-CSF (20 ng mL<sup>-1</sup>, 10 min., PeproTec Inc), IL-4 (10ng mL<sup>-1</sup>, 10 min., PeproTec Inc #300-03), INFα (1570 U mL<sup>-1</sup>, 10 min., PBL interferon source #11200), EGF (20 ng mL<sup>-1</sup>, 15 min., Sigma-Aldrich #9644) or medium with 20% serum for 15 min. Small molecule inhibitors were added 2 hours before and during stimulation. PD98059 (20µM Cell Signaling #9900), Wortmannin (0,5µM Sigma-Aldrich #W1628), AG1478 (80nM, Invitrogen #PHZ1034) and AKT inhibitor VIII (10µM, Calbiochem #124018). Post-stimulation, cell-microsphere complexes were fixed with 1.5 % paraformaldehyde for 10 min., and washed once with PBS. Cells were pelleted at 450g for 5 min. and permeabilized with 70% methanol 4°C for minimum 30 min. Treated cells could be stored for up to 3 months in methanol at -20°C without significant epitope deterioration.

### **Flow cytometry analysis**

Fixed, permeabilized cell-microsphere complexes were stained as described by Schulz 2012 <sup>5</sup>. Primary antibodies diluted in 1% bovine serum albumine in PBS as a blocking buffer: anti-COL1 (1/100 ,Sigma-Aldrich #C2456), Phospho-(Tyr44/42) MAP kinase dilution (1/1000, Cell Signaling #9106). These rabbit primary antibodies were used: anti-FN (5 µg mL<sup>-1</sup>, Millipore #AB2047) anti-Laminin (1:100, Sigma-Aldrich #L9393), Phospho-Erk (1/200, Cell Signaling #4370), Phospho-Akt (1/200, Cell Signaling #4060) Phospho-Marcks (1/50, Cell Signaling #2741). Conjugated antibodies (BD Biosciences): Murine Phospho-(Tyr694) Stat5 Alexa Fluor 647 (1/20, #612599), Murine Phospho-(Tyr705) Stat3 Alexa Fluor 647 (1/20, #557815). Secondary antibodies (Invitrogen) dilution of 1/5000 (0.4 µg mL<sup>-1</sup>): goat anti rabbit Alexa Fluor 647 (#A21244), goat anti rabbit Alexa Fluor 488 (#A11008), goat anti mouse Alexa Fluor 488 (#A21235) or goat anti mouse Alexa Fluor 647 (#A21236). Propidium iodide (Sigma-Aldrich #P4864), DAPI (Sigma-Aldrich #D9542) or Hoechst (Sigma-Aldrich #B2261) was introduced together with the secondary antibody in a concentration of 1 µg mL<sup>-1</sup>, 1 µg mL<sup>-1</sup> and 0.6 µg mL<sup>-1</sup> respectively. All centrifugation steps were conducted at 390g for 2 min. Duration of staining was 30 min. in room temperature for both primary and secondary antibody.

Samples were analysed on BD FACSCalibur, FACS Aria or BD LSRFortessa (BD Biosciences).

Flow cytometry data was analyzed with Flow Jo, (Tree Star Inc) and in Cytobank® for the preparation of colour labelled histograms.

### **Kinetic signal transduction analysis**

Cells were put into suspension and microspheres introduced according to protocol described above. Cell-microsphere complexes were collected at 10, 30, 45, 60, 120, 240 and 540 min. by adding PFA and methanol as described above. Median fluorescence intensity was plotted according to increasing period of ECM/microsphere exposure. MCF10A and MDA-MB-231 cells were run in identical medium supplemented with 20 ng mL<sup>-1</sup> EGF during the experiment in order to keep the stimulation input similar, while wild type and transformed HMEC were cultured in M87 complete medium containing 5 ng mL<sup>-1</sup> EGF. Signaling levels were normalized by calculating percentage of signaling in sample out of maximum signaling obtained in the given cell line on the three different ECM. Signaling levels were defined as sample fluorescence minus fluorescence of a sample stained with secondary antibody only. MCF10A and MDA-MB-231 samples were run on BD FACSCalibur (BD Biosciences). HMEC samples were run on BD LSRFortessa (BD Biosciences).

### **Confocal microscopy**

Cells adhered to COL1-coated microspheres and cells cultured on COL1 coated cover slips (COL1 100 µg mL<sup>-1</sup>) were fixed in 2% paraformaldehyde for 10 min, washed with PBS and permeabilized with 0.1% Triton X-100 for 10 min. followed by a double washing step and staining with Alexa Fluor 488 conjugated phalloidin (1/40 = 7.5 U mL<sup>-1</sup>, Invitrogen #A12379) for 20 min, after which they were washed 3 times in buffer. Cells on microspheres were resuspended in maximum 30 µL Triton buffer. A droplet was placed on a microscope slide, permitted to dry, then mounted with ProLongGold (Invitrogen #P36935) with DAPI for nucleus staining with a coverslip on top. Specimen was run on NIKON TE2000 and analyzed in 3D image analysis software IMARIS 6.3 to create TIFF images (Imaris snapshot) from Z-stacks.



### **Analysis of patient ovarian carcinoma cells in ascites fluid**

*Differential trypsination:* Ascites fluid collected from consenting ovarian carcinoma patients at the Haukeland University Hospital was kindly provided by Dr. Line Bjørge. Preferential adherence of fibroblasts to cell culture plates versus epithelial was used to deplete fibroblasts from cell culture as described<sup>30</sup>. The ascites sample was added to tissue culture plates and incubated at 37°C for 30 min. Adhered fibroblasts were discarded and unbound epithelial cells were reseeded into a fresh tissue culture plates. Cell detachment was monitored by microscopy. Detached fibroblasts were collected in a separate dish to confirm their identity. The remaining epithelial cells were washed with PBS and cultured in M87A complete medium<sup>13,14</sup>.

*Selective sorting of epithelial cells:* Cells from ascites fluid could also be sorted according to EpCam FITC positivity (1/100, Abcam #ab8666). Cells were adhered to microspheres as described above and stained with rabbit antibody Phospho-AKT (1/200, Cell Signaling #4060) and/or mouse antibody Phospho-ERK (1/200 Cell Signaling #4370) followed by goat anti-rabbit secondary antibody conjugated to Alexa647 and goat anti-mouse secondary antibody conjugated to Alexa488.

### **Scanning electron microscopy**

Cells treated according to protocol above were resuspended in fixative (2% gluteraldehyde in Sørensen's phosphate [PB] buffer) at room temperature followed by overnight fixation at 4°C. Gluteraldehyde was removed after a 500g spin down and the pellet was washed 3 times in PB buffer. Pellet was treated with 1% Osmium tetroxide for 1h followed by another 3x wash in PB buffer. Sample was dehydrated in an ascending alcohol series: 70, 96 and 100%, for 20 min in each bath. Sample was eventually put on stubs and dried over night at 37°C. Finally, the sample was coated with gold/palladium and imaged on Jeol JSM-7400F scanning electron microscope. Images were pseudocolored in Photoshop.

## Acknowledgements

We kindly thank Dr. Iren Abrahamsen for important recommendations on the experimental protocols; Dr. Martha Stampfer for contributing breast tissue from collected tissue samples and instructions in how to care for these cells; Marianne Enger and Sissel Vik Berge for technical assistance; Dr. Line Bjørge at Kvinneklinikken for providing ovarian cancer patient ascites samples; and the peer-reviewers for helpful comments on the manuscript. H.E was supported by a Norwegian Cancer Society predoctoral fellowship and travel grant. J.B.L is supported by grants from the Norwegian Research Council, Norwegian Cancer Society and Helse Vest Health Authority.

## References

- 1 K. R. Levental, H. Yu, L. Kass, J. N. Lakins, M. Egeblad, J. T. Emler, S. F. T. Fong, K. Csiszar, A. Giaccia, W. Weninger, M. Yamauchi, D. L. Gasser and V. M. Weaver, *Cell*, 2009, **139**, 891–906.
- 2 M. LaBarge, C. M. Nelson, R. Villadsen, A. Fridriksdottir, J. R. Ruth, M. R. Stampfer, O. W. Petersen and M. J. Bissell, *Integr. Biol. (Camb)*, 2009, **1**, 70–79.
- 3 A. P. Gilmore, *Cell Death Differ.*, 2005, **12**, 1473–1477.
- 4 R. O. Hynes, *Cell*, 2002, **110**, 673–687.
- 5 K. R. Schulz, E. a. Danna, P. O. Krutzik and G. P. Nolan, *Curr. Protoc. Immunol.*, 2012, 1–20.
- 6 J. Irish, N. Kotecha and G. P. Nolan, *Nat. Rev.*, 2006, **6**, 9.
- 7 M. D. Frame and I. H. Sarelius, 2000, 419–427.
- 8 P. O. Krutzik and G. P. Nolan, *Cytometry. A*, 2003, **55**, 61–70.
- 9 S. D. Schimmel, G. R. Grotendorst and R. I. Grove, *Cancer Lett.*, 1980, **9**, 229–236.
- 10 C. A. Weston and B. S. Weeks, 1996, **323**, 318–323.
- 11 T. Tiganis, B. E. Kemp and N. K. Tonks, *J. Biol. Chem.*, 1999, **274**, 27768–27775.
- 12 J. K. Lee, J. C. Garbe, L. Vrba, M. Miyano, B. W. Futscher, M. R. Stampfer and M. LaBarge, *Front. Cell Dev. Biol.*, 2015, **3**, 1–9.
- 13 M. Stampfer, R. C. Hallows and A. J. Hackett, *In Vitro*, 1980, **16**, 415–425.
- 14 J. C. Garbe, S. Bhattacharya, B. Merchant, E. Bassett, K. Swisshelm, H. S. Feiler, A. J. Wyrobek and M. R. Stampfer, 2009, 7557–7568.
- 15 E. Mattila, T. Pellinen, J. Nevo, K. Vuoriluoto, A. Arjonen and J. Ivaska,

- Nat. Cell Biol.*, 2004, **7**, 78–85.
- 16 M. a Schwartz and M. H. Ginsberg, *Nat. Cell Biol.*, 2002, **4**, E65–E68.
  - 17 K. M. Yamada and S. Even-ram, *Nat. Cell Biol.*, 2002, **4**, E75–76.
  - 18 M. C. Mendoza, E. Emrah Er and J. Blenis, *Trends Biochem*, 2011, **36**, 320–328.
  - 19 S. Zimmermann and K. Moelling, *Science*, 1999, **286**, 1741–1744.
  - 20 C. . Hong, T. Kume and R. . Peterson, *Circ Res*, 2008, **104**, 573–579.
  - 21 M. Hellesøy and J. B. Lorens, *Mol Biol Cell*, 2015, **May 28**.
  - 22 R. P. Wersto, F. J. Chrest, J. F. Leary, C. Morris, M. Stetler-stevenson and E. Gabrielson, 2001, **306**, 296–306.
  - 23 W. Buchser and D. Ph, 2014.
  - 24 B. Bodenmiller, E. R. Zunder, R. Finck, T. J. Chen, E. S. Savig, R. V Bruggner, E. F. Simonds, S. C. Bendall, K. Sachs, P. O. Krutzik and G. P. Nolan, *Nat. Biotechnol.*, 2012, **30**, 857–866.
  - 25 M. D. Leipold and H. T. Maecker, 2012, 2–12.
  - 26 P. Pozarowski, E. Holden and Z. Darzynkiewicz, 2014, 187–212.
  - 27 A. H. C. Ng, M. D. Chamberlain, H. Situ, V. Lee and A. R. Wheeler, *Nat. Commun.*, 2015, **6**, 1–12.
  - 28 J. Debnath, S. K. Muthuswamy and J. S. Brugge, *Methods*, 2003, **30**, 256–268.
  - 29 R. Cailleau, R. Young, M. Olivé and W. J. Reeves, *J. Natl. Cancer Inst.*, 1974, **53**, 661–674.
  - 30 M. Labarge, J. C. Garbe and M. R. Stampfer, *J. Vis. Exp.*, 2013, 1–7.
  - 31 S. Swift, J. Lorens, P. Achacoso and G. P. Nolan, 2001, UNIT 10.17C.
  - 32 A. Boyum, *Scand. J. Clin. Lab. Invest.*, 1982, **21**, 1982.
  - 33 I. Abrahamsen and J. B. Lorens, *BMC Cell Biol.*, 2013, **14**, 36.

## Figure legends

**Fig. 1. The microsphere cytometry approach to measure adherent cell signaling at the single cell level** (A) Scanning electron microscopy images exemplifying different stages of a mammary epithelial MCF10A cell adhering to an ECM-coated microsphere. (B) Schematic representation of the microsphere cytometry approach. (C) Flow cytometry gating strategy to resolve microspheres, unbound cells and microsphere-bound cells by DNA staining and granularity. Phase-contrast images of the three flow sorted populations. (D) Comparison between the unbound and bound population shows an identical distribution of > 4n DNA content, indicating that one cell

adheres per microsphere. (E) Cell adhesion kinetics for binding of MCF10A to different ECM presented as percentage of microsphere-bound cells within a population. (F) Microsphere cytometry analysis of pERK levels in serum and phorbol ester (PMA) treated NIH3T3 fibroblasts adhered to COL1-coated microspheres. Flow data are presented in fluorescence intensity. Bar represents 20  $\mu\text{m}$ .

**Fig. 2. Simultaneous measurement of cell signaling responses in adherent and non-adherent monocytes by microsphere cytometry**

U937 and primary human CD14<sup>+</sup> monocytes were treated with FGF2 (20 ng mL<sup>-1</sup>) to induce adhesion to FN-coated microspheres. Mixed microsphere-bound, unbound cells or suspension cells alone were growth factor/cytokine stimulated and cell signaling changes analyzed by flow cytometry. Gating strategy is shown in dot plots on the left. (A) Adherent and suspension U937 cells and (B) primary human monocytes were stimulated with PMA (50  $\mu\text{M}$ , 2 min.), FGF2 (100 ng mL<sup>-1</sup>, 15 min.), GM-CSF (20 ng mL<sup>-1</sup>, 10 min.) and IL-6 (20 ng mL<sup>-1</sup>, 10 min.). Phospho-proteins tested: ERK, MARCKS, AKT, Stat5 and Stat3. Median fluorescence intensity color scale is shown. Control samples were stained with secondary antibody only. Representative of two independent experiments.

**Fig. 3. Contextual cell signaling responses to ECM in mammary epithelial cells.** pERK and pAKT signaling in MCF10A cells adhered to COL1, COL4, FN, VN and LAM coated microspheres in response to treatment with EGF (20 ng mL<sup>-1</sup>, 10 min.), PMA (50 nM, 2 min.) or serum (5%, 2 min.). Color scale indicates the log<sub>2</sub> value of phospho-protein levels upon stimulation compared to basal phosphorylation levels. pERK: top row; pAKT: bottom row. Basal phosphorylation measured following treatment with inhibitor compounds: pAKT, wortmannin (0.5  $\mu\text{M}$ , 2 hours); pERK, PD98059 (10  $\mu\text{M}$ , 2 hours). Representative of three independent experiments.

**Fig. 4. Microenvironment-dependent cell signaling response patterns distinguish normal and neoplastic cells.**

pERK and pAKT levels were measured longitudinally in mammary epithelial and carcinoma cells (HMEC, HMEC/Neu, MCF10A, MDA-MD-231) adhered to COL1, FN or LAM-coated microspheres in growth factor supplemented culture medium. (A) Examples of pERK histograms in response to EGF in HMEC and HMEC/Neu cells bound to COL1. (B) Contour plots of temporal (10 min - 2 hr) pERK/pAKT levels in MCF10A cells bound to FN-coated microspheres. (C-E) MFI (median fluorescent intensity) values for pERK (solid lines) and pAKT (dotted lines) plotted as a function of time. (C) Cell signaling in cells without the presence of ECM or growth factors. (D) 0-2 hr; (E) 0-9 hr. Background fluorescence signal was determined by staining with secondary antibody only; this was subtracted from the sample MFI values. Values were plotted as the ratio of the maximum value of pERK or pAKT level in the kinetic series on a given ECM. Representative of three independent experiments.

**Fig. 5. Microsphere cytometry reveals inter-relationships between adherent cell signaling pathways.**

(A) pAKT and pERK levels in MCF10A cells adhered to COL1, FN or LAM-coated microspheres were measured before and after stimulation with EGF (20 ng mL<sup>-1</sup>) or PMA (50nM) in the presence of (B) EGFR inhibitor AG1479 (80 nM), (C) PI3 kinase inhibitor Wortmannin (500 nM), (D) AKT inhibitor VIII (10 μM) or (E) MAP kinase inhibitor PD98059 (10 μM). Control samples were stained with secondary antibody only. Log<sub>2</sub> values of shift in MFI of sample population compared to control is presented as color-coded histograms. Representative of three independent experiments.

**Fig. 6. Microsphere cytometry analysis of primary tumor biopsies.**

Ovarian carcinoma cells were enriched from patient ascites fluid by (A) FACS sorting for EpCam expression or (B) by seeding into tissue culture plates and differential trypsinization. Phospho-protein (pAKT and pERK) analysis of the resulting cell population growth was performed. (A) EpCAM<sup>+</sup> cells were adhered to LAM coated microspheres, stimulated with EGF and pERK activation measured by flow cytometry. (B) Ovarian carcinoma cells enriched by differential trypsinization were adhered to COL1 coated microspheres pERK levels were monitored over time. Bars. 30 μm.

Suppl. Table 1. MFI changes for pERK and pAKT for each condition tested in Figure 3. Log<sub>2</sub> value of phospho-protein levels upon stimulation compared to basal phosphorylation levels is shown.

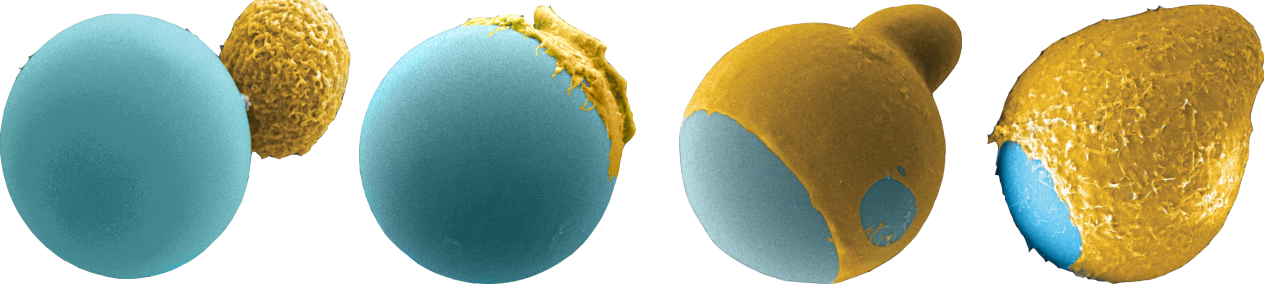
**Suppl. Fig. 1.** (A) Confocal microscopy analysis of phalloidin-stained MCF10A cells adhered a COL1-coated microsphere or a tissue culture surface (Z stack projection). Dotted circle indicates microsphere circumference. (C) Kinetics of MDA-MB-231 cell adhesion to COL1, LAM or FN. (D) Flow cytometry analysis of microspheres shows uniform ECM protein coating. Bar: 10  $\mu$ m.

**Suppl. Fig 2.** Cell morphology is context dependent. Human mammary epithelial cells (HMEC) adopt different morphologies when adhered to different ECM matrices. Bar: 30 $\mu$ m.

**Suppl. Fig. 3.** CD227 analysis of partially trypsinized ovarian carcinoma cells from patient ascites fluid. Control is (unstained) cell autofluorescence.

Suppl. Movie 1. . Animation of Z stack projection.

**A** Figure 1



**B** adherent cells grown on a tissue culture dish

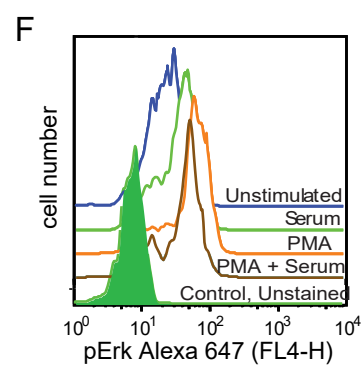
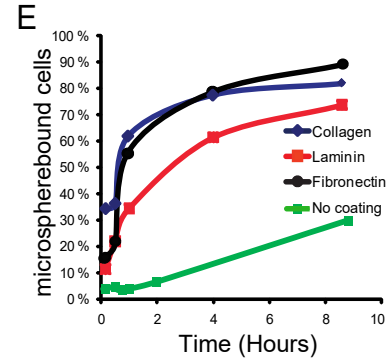
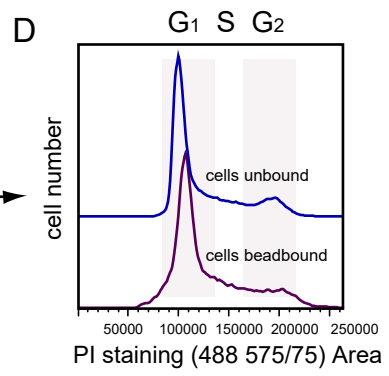
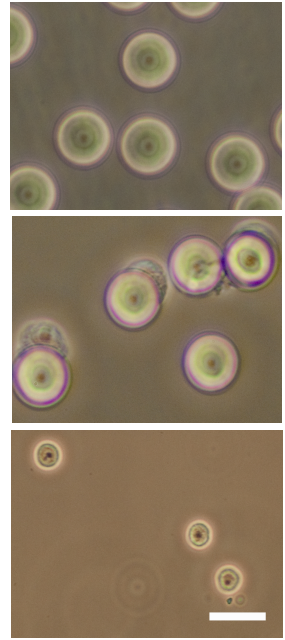
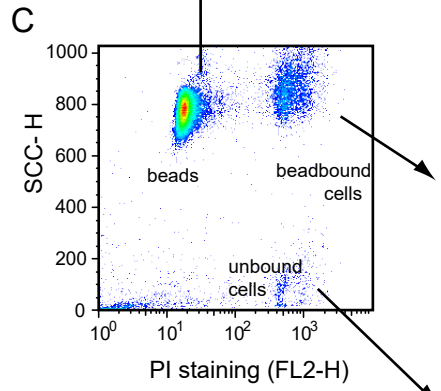
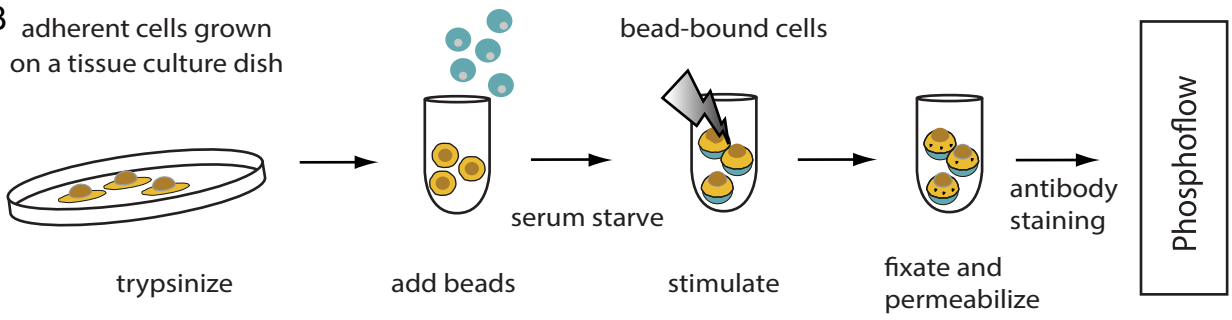
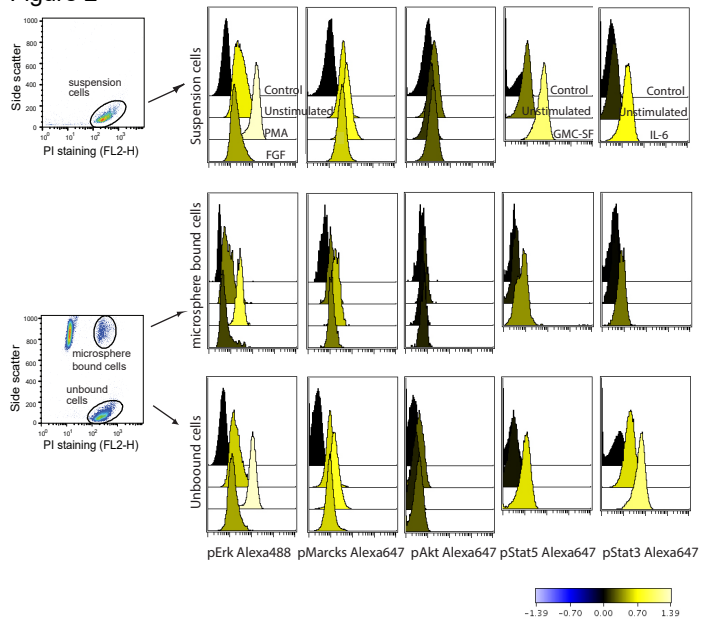
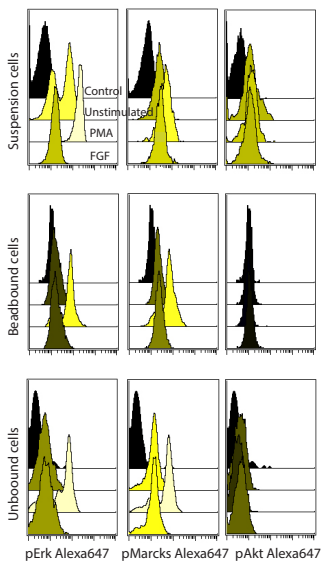


Figure 2



**B Primary monocytes**





Uncoated

Collagen I

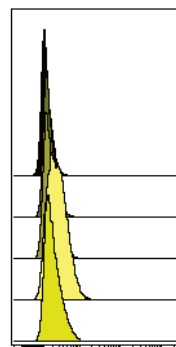
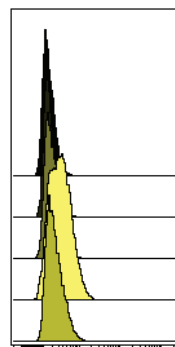
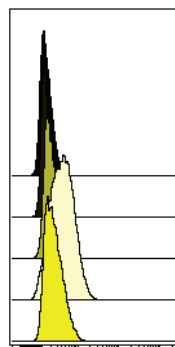
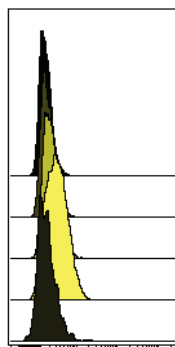
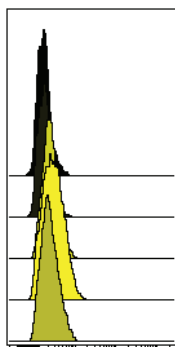
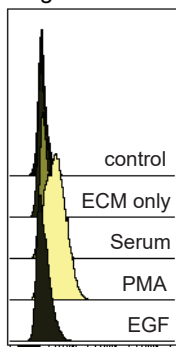
Collagen IV

Fibronectin

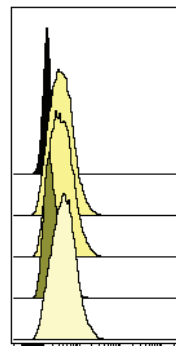
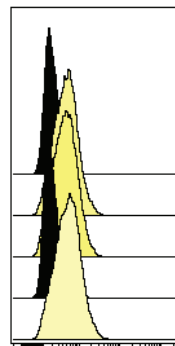
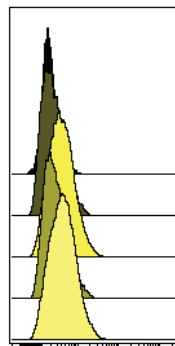
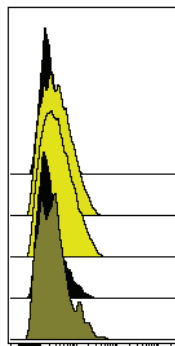
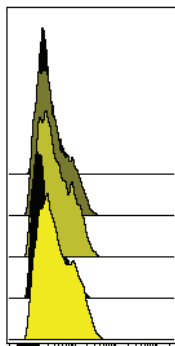
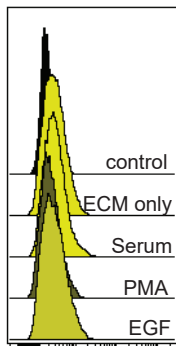
Vitronectin

Laminin

Figure 3



pERK Alexa 488-A



pAKT Alexa 647-A

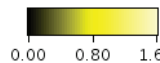
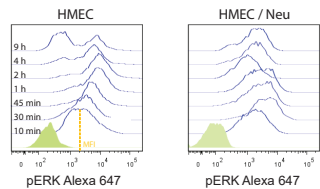
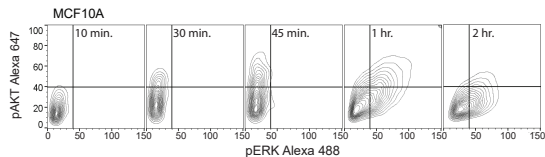


Figure 4

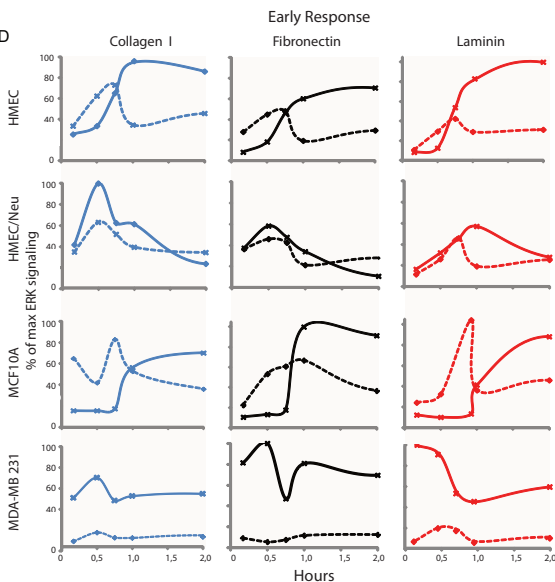
A



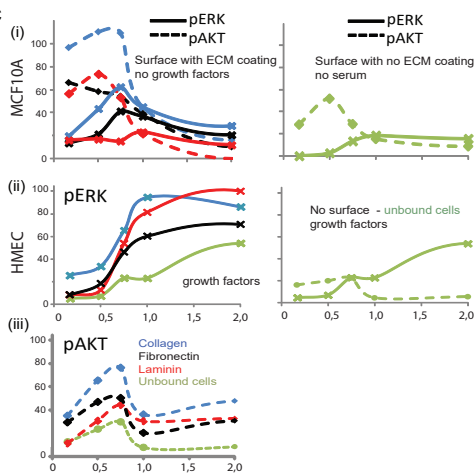
B



D



C



E

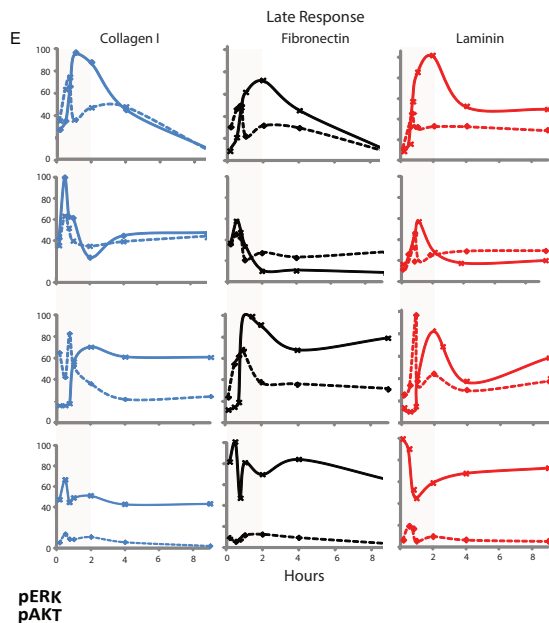


Figure 5

pERK

pAKT

Collagen

Fibronectin

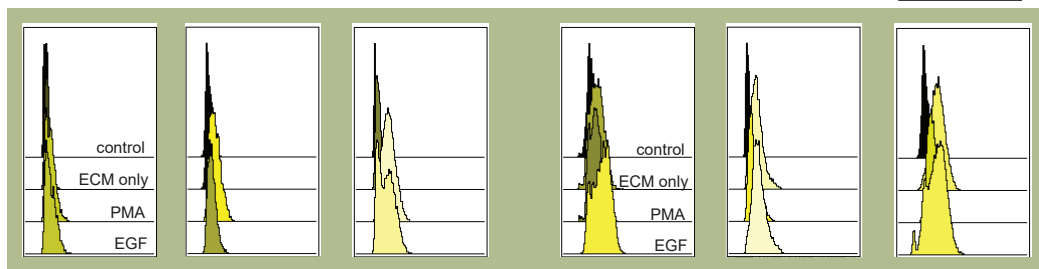
Laminin

Collagen

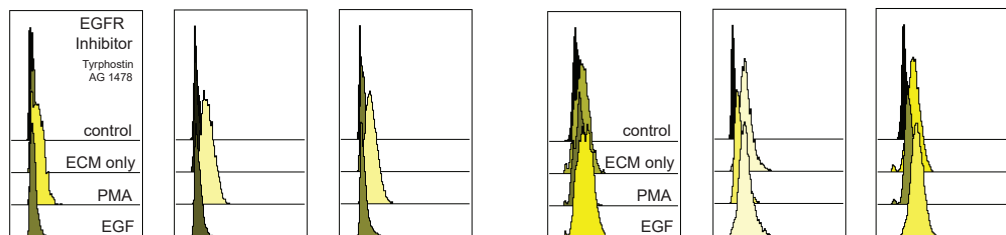
Fibronectin

Laminin

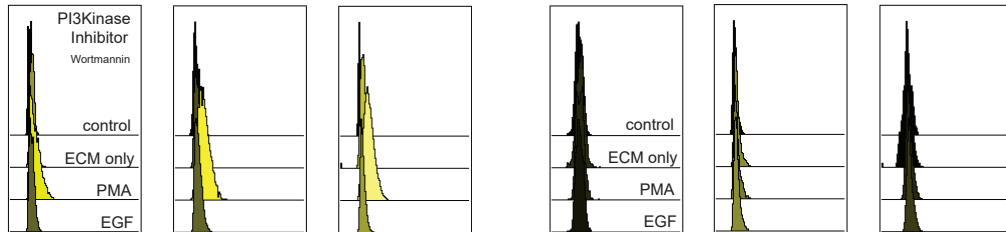
A



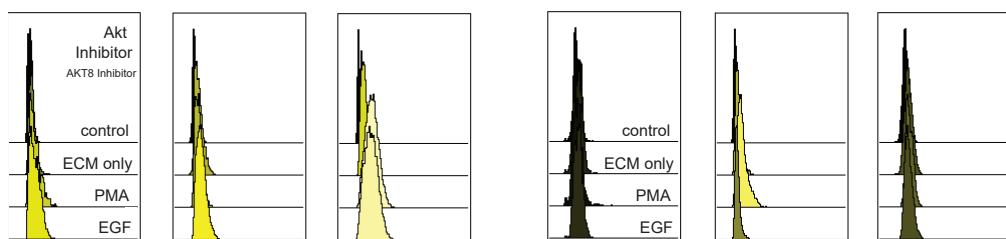
B



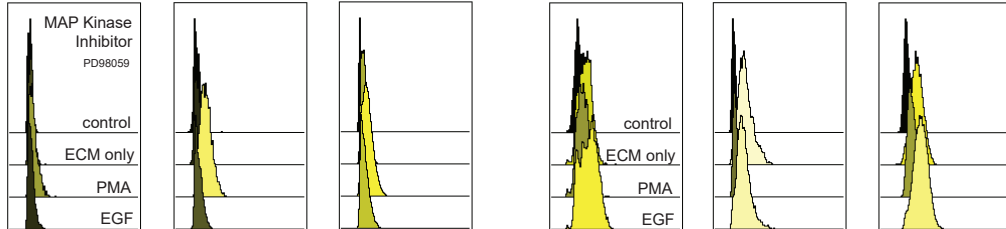
C



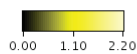
D



E

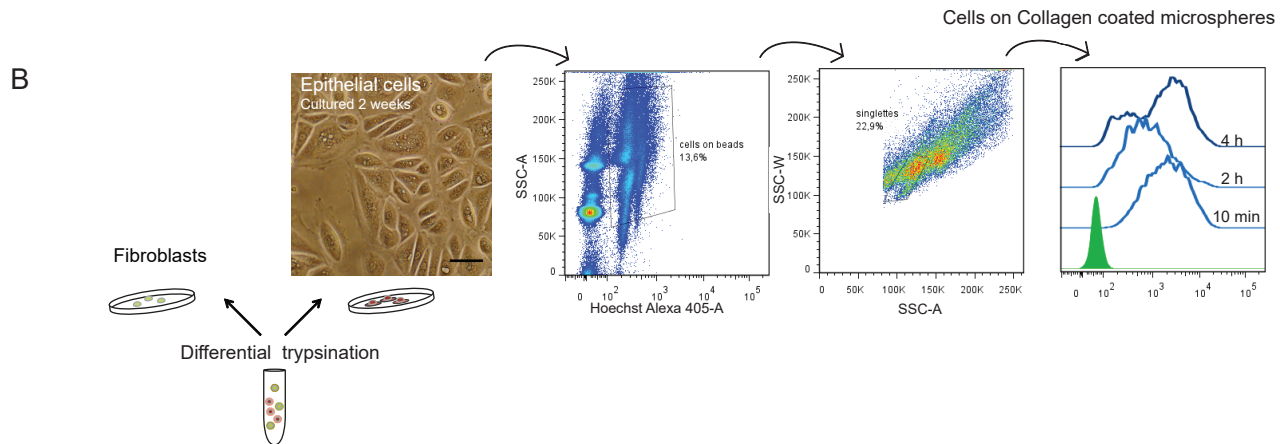
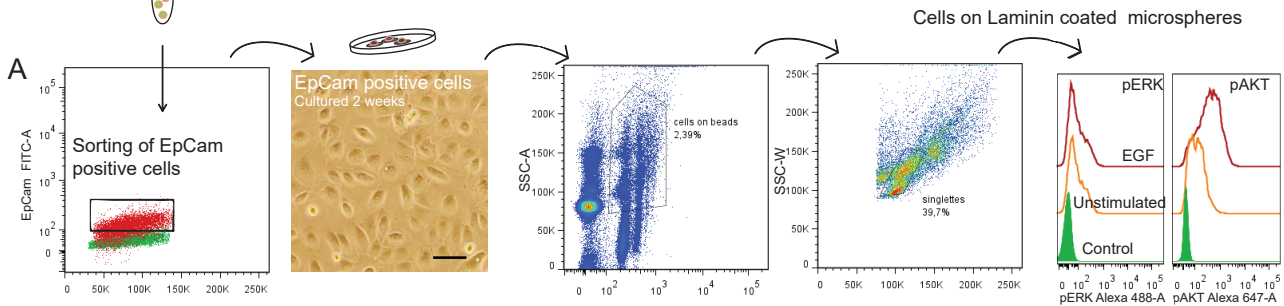


Alexa488-A



Alexa647-A

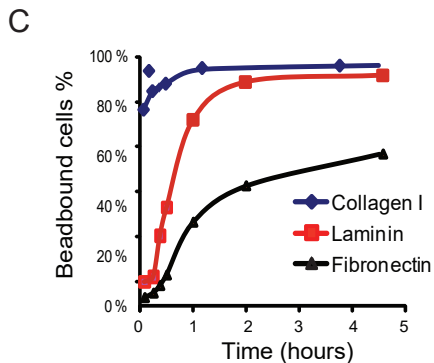
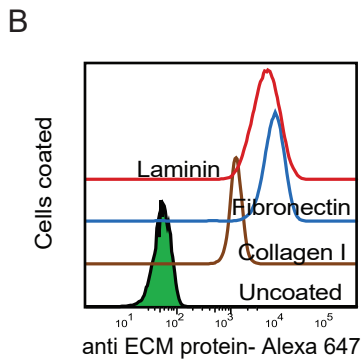
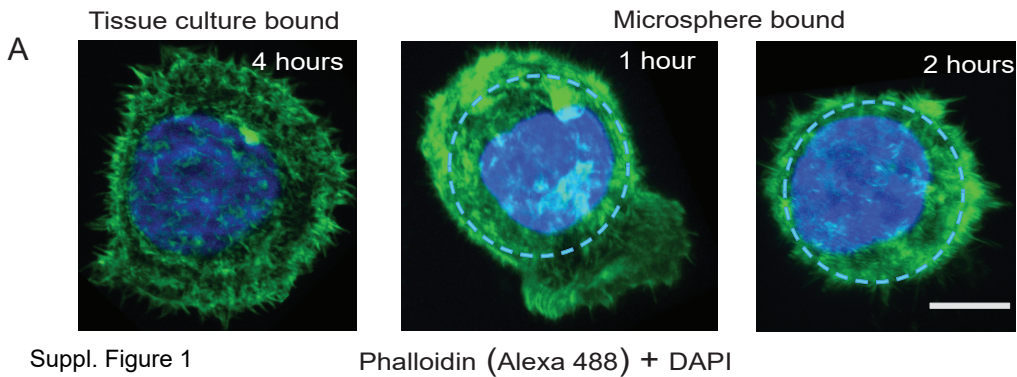
Figure 6



<b>pERK</b>	Uncoated	Collagen I	Collagen IV	Fibronectin	Vitronectin	Laminin
Control	0	0	0	0	0	0
ECM only	0.11	0.08	0.21	0.06	0.11	0.35
Serum	0.43	0.66	0.59	0.56	0.38	0.51
PMA	1.4	0.95	1.14	1.61	1.21	1.22
EGF	0.09	0.58	0.09	0.77	0.58	0.7


Suppl. Table 1

<b>pAKT</b>	Uncoated	Collagen I	Collagen IV	Fibronectin	Vitronectin	Laminin
Control	0	0	0	0	0	0
ECM only	0.70	0.38	0.70	0.27	1.35	1.37
Serum	0.71	0.60	0.71	1.10	1.26	1.36
PMA	0.30	- 0.26	0	0.51	- 0.02	0.45
EGF	0.63	0.78	0.40	1.25	1.52	1.61

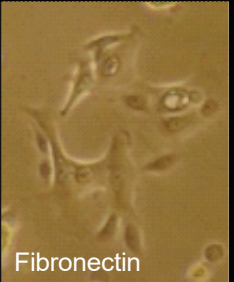


Suppl. Figure 2

Collagen I



Fibronectin



Laminin



Suppl. Figure 3

